Int J Epidemiol Health Sci 2024;5: e67
doi: http//doi.org/10.51757/IJEHS.5.2024. 711131

Original article

Numerical Analysis of the Sixth to Eighth Waves of the COVID-19 Epidemic in Tokyo, Including Control over the Number of People Tested for Outbreak Suppression (6th to 8th COVID-19 Waves in Tokyo and Countermeasure)

Kyosuke Ono [1,*] and Katsuaki Kikuchi [2]

[1] Emeritus Professor of Tokyo Institute of Technology, Tokyo, Japan.
[2] Former Engineer of Hitachi Co., Ltd., Ibaraki-prefecture, Japan.

***. Corresponding author:** Kyosuke Ono, Emeritus Professor of Tokyo Institute of Technology, Tokyo, Japan. Email: ono_kyosuke@nifty.com.

Cite this article: Ono, K., Kikuchi, K. Numerical Analysis of the Sixth to Eighth Waves of the COVID-19 Epidemic in Tokyo, Including Control over the Number of People Tested for Outbreak Suppression (6th to 8th COVID-19 Waves in Tokyo and Countermeasure). Int J Epidemiol Health Sci 2024;5:e67. Doi: 10.51757/IJEHS.5.2024.711131.

Abstract

Background: It is extremely important to use existing data to study the transition of infection and removal rates, as well as the influence of vaccination, in the major epidemic waves 6, 7, and 8 in Tokyo, and to develop an effective countermeasure to suppress the epidemic.

Methods: We developed a new *IR* model of the epidemic in which *I* and *R* comprise both symptomatic and exposed individuals. Based on this model, numerical methods were developed to calculate infection and removal rates, as well as the vaccine effect. To minimize the maximum number of daily positives R_d, we developed a mechanism for controlling the number of people examined *T* based on the R_d rate.

Results: The transitions between epidemic waves 6 and 8, as well as the overall vaccination effect in reducing infection rates, were clarified. Using the measured link between removal rate and tested individuals, the suppressive impact of *T* control was recreated for waves 6 to 8. As a result, wave 6 showed a significant drop in the maximum R_d from one tenth to one half of the actual data. Although the test system was greatly reinforced in waves 7 and 8, the *T* control was still able to cut the maximum R_d in half when implemented within 10 days of the epidemic waves' onset.
Conclusion: The novel *IR* theory, the calculation method for predicting infection and removal rates, and the *T* control will all give formidable instruments for future epidemic suppression.

Keywords: COVID-19, Epidemiological model, Epidemic wave analysis, Vaccination effect, Tested people number control, Epidemic countermeasure, Japan

Introduction

Due to the invasion of novel coronavirus COVID-19 infection from abroad, Japan experienced epidemic waves 1 and 2 in 2020, waves 3, 4, and 5 in 2021, and waves 6, 7, and 8 from January 2022 to February 2023. The 8th wave of omicron variations had a fatality rate comparable to influenza, and the novel coronavirus COVID-19 infection was reduced to Class 5, the same as seasonal flu, on May 8, 2023. A ninth wave of infectious epidemics occurred between April and September, followed by a period of contraction.
Because the 7th mRNA vaccination is now free of charge, the epidemic is no longer as serious as it was before the 8th wave. However, as of November 2023, about half of Tokyo residents continue to live the current lifestyle and wear masks when they go out. The worst waves of COVID-19 infection in Japan occurred in the sixth, seventh, and eighth waves,

when the number of daily positive cases in Tokyo was 3.6, 6.6, and 3.5 times higher than the peak of the fifth wave of delta strains, respectively (1).

A state of emergency was declared in Japan beginning with the first wave of the outbreak as the number of sick people surged and the administrative inspection and medical systems became overwhelmed. In contrast, several infectious disease epidemiologists have emphasized the necessity of large-scale inspections, which have proven effective in Korea, Taiwan, and other countries (2,3).

We are not experts in infectious disease epidemics, but as mathematical analysis experts in engineering, we have argued, based on a simple SIR model of COVID-19 infection, that rapid expansion of testing and isolation is a cost-effective and efficient measure that can prevent the spread of infection while maintaining social and economic activities, rather than political regulation of social and economic activities (4). We examined the 5th wave, which occurred around the Tokyo Olympics game, and discovered that the half of the number of tests owing to consecutive holidays between the Olympics' opening and closing activities was the primary reason of the unanticipated spread of infection (5). It was also demonstrated that the increase in mRNA vaccination rate, which occurred concurrently with the spread of infection, contributed to the drop in infection after mid-August 2021 (6).

In this study, we first propose a simple ***IR*** theory that is appropriate for the analysis of COVID-19 outbreaks, where ***I*** represents all positive cases, including exposed and symptomatic individuals, and ***R*** represents the removal of all positive cases by testing. utilizing this theoretical model, we next quantitatively examined the changes in the number of infected people in the city, the infection rate, and the removal rate during the 6th, 7th, and 8th waves of the epidemic in Tokyo, utilizing data from daily reports of positive cases (7). The association between the number of persons tested and the removal rate in each wave was also explained. The role of vaccination in lowering infection rates in each wave of the epidemic was also evaluated.

To limit the spread of illness as rapidly as feasible, we suggest a T control mechanism in which the number of persons tested T increases in proportion to the number of daily positives R_d. The efficiency of the T control approach was subsequently proved by simulation analysis, which used regression equations for the removal rate and the number of persons evaluated in each wave.

Materials and Methods

Data acquisition of infectious status in Tokyo and processing

Figure 1 shows the infection status data published by the Tokyo Metropolitan Government (TMG) (7) from November 10, 2020, to February 28, 2023. The TMG publishes the number of daily positives by testing date, reported date, and verified date. The R_d is the number of daily positives on the day when the PCR and antigen testing were completed in the laboratories and the findings were available. R_{dr} is based on the date the infection was reported to the public health center and is a preliminary statistic that is provided as the number of new daily positives. R_{dc} represents the number of daily positives arranged by the day the physician confirmed the positivity. However, as R_{dc}'s publishing terminated on September 25, 2022, only R_{dr} is shown after that, which is nearly identical to R_{dc}. The TMG has published the sum of the number of persons tested for PCR and antigen as the number of persons tested T and the value of R_d/T as the positive rate (φ). Figure 1 shows the T and φ. These are moving averages for the last seven days. This paper's infection study focuses on the link between the T and the R_d.

As shown in Figure 1, the number of R_d forms waves 3 to 8. The duration of each wave, the total number of days in the period, the total number of R_d, the maximum number of R_d, the total number of deaths, and the fatality rate are shown in the inset table. The number of R_d is almost the same as R_{dc} until the 5th wave. After the 6$_{th}$ wave, however, the maximum values are significantly different, with R_{dc} being about 1.5 to 1.8 times higher than the R_d. The R_d includes only those who were confirmed by the laboratory, whereas the R_{dc} includes those who were confirmed by other medical facilities and is more representative of the true situation. The number of removed persons is low in waves 3 to 5, but increases in wave 6 and later waves. As shown in the inset table, the maximum value of R_d (R_{dr}) is 3, 822 (4,954) in the 5th wave, while it is 11,672 (17, 859) in wave 6, a significant increase of 3.1 (3.6) times. After the decline of the 5th wave, the R_d remained at about 20, but increased rapidly towards the end of the year and the beginning of the new year; on 1/1/2022, the R_d was 60 (R_{dc}: 70), but one-week later 1/8 (month/day), it jumped to 619 (744), a 10.3 (10.6) fold increase. In wave 7, the maximum value of R_d was 18,429, which was 1.58 times higher than in wave 6. In wave 8, the maximum number of R_d was 9,552, which was lower than the respective maximums of waves 6 and 7.

Looking at the changes in the variants of the new coronavirus shown in the upper part of Figure 1, the 5th wave was infected only with alpha and delta strains, but from the 6th wave onwards, the omicron strains have spread (8). The omicron strain is said to be 1.5 to 2 times more infectious than the delta strain, which is clearly a factor in the increase in the number of removed persons from wave 6 onwards. However, the fatality rate after wave 6 is lower than that of wave 5. This may be due to the high vaccination rate, especially among the elderly, and the improvement of the medical system.

On the other hand, the number of T should be proportional to the number of R_d to detect and isolate positives at an early stage, but since the T did not increase proportionally to R_d, the positivity rate φ also increased with the increase in R_d. For example, in wave 6, the maximum value of R_d increased approximately threefold compared to wave 5, while the number of T increased 1.8-fold, resulting in a 1.7-fold increase in φ. Although the testing system is in the early period of the spread is important to prevent the spread of infection, we can observe a clear reduction in the number of T during the New Year period at the beginning of wave 6, which is another reason for the rapid spread of infection in wave 6.

_IR_ theory for the analysis of COVID-19 infection

The theoretical model commonly used to analyze the expansion and contraction of infectious disease epidemics is the SEIR model shown in Figure 2(a) (9-12). Figure 2(a) shows the relationship between the susceptible population S, the number of people exposed to infection E, the number of symptomatically infected people I and the number of persons isolated by testing R. The SEIR model is based on the SIR model proposed by Kermack and McKendrick (13), which considers the incubation period or infectious disease onset period of exposed persons E. The characteristic feature of the SIR and SEIR theory is that the susceptible population S decreases and the epidemic naturally declines when infected persons I are removed from quarantine and the cumulative number of those who recover and become immune is greater than approximately 70% of S. However, in the case of a COVID-19 epidemic, the cumulative number of those who were removed as positive by quarantine was less than 6.6% of the total population $N = \sim 1.4\times10_7$, and the maximum daily removed person R was only 0.13%, even during the largest 7th waves of the epidemic. In addition, the majority of removed persons R recover with medical treatment, and the infection rate decreases to some extent due to immunity and returns to the susceptible population S. Therefore, the infection rate β^*S (β^* is the infection rate per person in S) for infected persons I hardly changes and can be regarded as a constant value $\beta_0 = \beta^*S$ in one wave of infection.

Figure 2(b) shows the $(E + I)R$ model used in this paper, which also takes into account the vaccination effect. First, the infection rate in terms of infected persons I in the absence of vaccination is $\beta_0 (= \beta^*S)$. If the number of vaccinated persons is $V(t)$ and the effective rate at which the vaccine reduces the infection rate is $\zeta(t)$, then the infection rate β in S is $\beta = \beta^*(S - \zeta * V) = \beta^*S(1 - \zeta * V/S) \approx \beta_0(1 - \zeta * V/N_p) = \beta_0(1 - \xi)$, where the asterisk represents the convolution integral of the vaccination rate $\zeta(t')$ and $V(t)/N_p$, ξ is the effective vaccination rate and the effective rate of reduction of β relative to the infection rate β_0 in the absence of vaccination because $\xi = (\beta_0 - \beta)/\beta_0$.

Next, among the susceptible people S, including the vaccinated, the exposed persons E is known to be capable of infection within the incubation period. Therefore, if the effective infection rate for asymptomatic and symptomatic positive persons $(E+I)$ is denoted by β, the rate of increase of E is given by the following equation, because the positive persons $E+I$ generate a newly infected exposed persons E.

$$dE/dt = \beta(E + I) - \epsilon E \qquad \text{Equation 1}$$

where ε is given by $\varepsilon = 1/d$ if the incubation time for E to become I is d days. The mean incubation time for alpha strains has been reported to be ~5 days and the mean infectious acquisition time to be 4.6 days (14,15), but this was later reduced to $d = \sim 4.4$ days for 5th wave delta strains and $d = \sim 3.6$ days for omicron strains as the mean incubation time (16). he infectious acquisition time is estimated to be further reduced by about 1 day. On the other hand, the number of symptom-positive persons I is assumed to increase by εE per unit time and to decrease by $E+I$ multiplied by the removal rate γ by testing. Thus, we have

$$dI/dt = \epsilon E - \gamma(E + I) \qquad \text{Equation 2}$$

Because the removed persons R includes not only symptomatic persons but also asymptomatic persons according to the tests, including the close contacts, the rate of increase of R is given by:

$$dR/dt = \gamma(E + I) \qquad \text{Equation 3}$$

In conventional SEIR theory, only symptomatic persons I have been considered as infectious persons in Equation 1 and removed persons in Equations 2 and 3. In reality, however, it is more reasonable to consider all positive persons $(E + I)$ as infectious persons and removed persons. Because the removed persons as daily positives by testing include asymptomatic persons, it is reasonable to consider the

removal rate γ as a coefficient of $(E+I)$. On the other hand, because the infectivity $\beta(E+I)$ includes superspreaders with high infectivity, asymptomatic but infectious persons and persons with zero infectivity immediately after exposure, it is reasonable to consider the infection rate β as an additive average of these.

By summing both sides of Equations 1 and 2, we obtain:

$$d(E+I)/dt = (\beta - \gamma)(E+I) \quad \text{Equation 4}$$

Thus, if all positives $(E+I)$ of asymptomatic and symptomatic persons are denoted as $\boldsymbol{I}(t)$, equations 4 and 3 become Equations 5 and 6, respectively:

$$d\boldsymbol{I}/dt = \{\beta(t) - \gamma(t)\}\boldsymbol{I}(t) \quad \text{Equation 5}$$

$$d\boldsymbol{R}/dt = \gamma(t)\boldsymbol{I}(t) \quad \text{Equation 6}$$

That is, by defining the sum of exposed, asymptomatic, and symptomatic persons for $\boldsymbol{I}$ and $\boldsymbol{R}$, and defining the average infection rate β and removal rate γ for these $\boldsymbol{I}$ and $\boldsymbol{R}$, the dynamics of infected and removed persons based on daily positive data can be mathematically captured by a simple new ***IR*** model.

Furthermore, in Figure 2(b), if ω is the fatality rate of medical deaths among the removed persons R, then the number of deaths is $D = \omega R$, where $(1-\omega)R$ is the number of persons who recovered and returned to S after a treatment period. The recovery period varies from as little as a week to as much as a month or more, but at least by the start of the next epidemic wave, most of the cumulative number of R can be assumed to have recovered to a new susceptible S. Because the daily maximum of R is less than 20 000 even in the 7th wave, the largest, it can be assumed that S in the new wave is almost unchanged from N_p (= ~14 million), considering that this corresponds to the period of vaccine efficacy. In the ***IR*** theory described above, $N_p = S + \boldsymbol{I} + \boldsymbol{R} + D$ always holds, and the number of vaccinees V is considered as a reduction of the effective infection rate in the same susceptible people S.

Next section describes a mathematical method for calculating the changes in infected persons $\boldsymbol{I}$, the infection rate β and the removal rate γ from the actual daily data of positive persons R_d, based on the theoretical ***IR*** model with Equations 5 and 6. Later, it will be described a method for calculating the effective vaccination rate.

Determination of the infectious rate β and removal rate γ

According to the mathematical model of infection in Equations 5 and 6, the number of infected persons I changes exponentially, and if γ is assumed to be constant in each interval, then the change in R_d is also assumed to be exponential in that interval. When the R_d is plotted on a logarithmic graph, if there is an interval where the slope is almost constant, then R_d can be considered to change exponentially with β and γ being constant. Therefore, the whole period is divided into many intervals in which β and γ are assumed to be constant. For each interval i, we can choose the sampled dates from t_{i1} to t_{in} and the corresponding n actual values of R_{dij}. Then, the following calculation is performed for interval i.

1) Assuming initial values of the variables β and γ, R^*_{dij} is calculated for each day t_{ij} according to the mathematical model of infection by equation 5 and 6,

2) Let Δ_{ij} be the deviation between the calculated value R^*_{dij} and the actual value R_{dij}:

$$\Delta_{ij} = R^*_{dij} - R_{dij} \quad \text{Equation 7}$$

The sum of squares of the deviation Δ_{ij} over the interval i is calculated:

$$\Delta = \sum_{j=1}^{n} \Delta_{ij}^2 = \sum_{j=1}^{n} (R^*_{dij} - R_{dij})^2 \quad \text{Equation 8}$$

3) The above calculation is repeated by changing the variables β and γ so that Δ is minimized,

4) Considering that the removal rate γ varies with the number of persons tested T, the following constraints are imposed on the calculated γ_i using the actual value of T_i in interval i and T_{i-1} in interval i-1.

$$\gamma \geq \gamma_{i-1} \quad if \quad T_i - T_{i-1} \geq 0 \quad \text{Equation 9}$$

$$\gamma < \gamma_{i-1} \quad if \quad T_i - T_{i-1} < 0 \quad \text{Equation 10}$$

5) Let β_i and γ_i in the interval i be the solutions of β and γ when Δ in equation 8 converges to a given minimum value by iterating through the above steps 1) to 4).

The above calculations are performed for all intervals to obtain β and γ for the entire period under consideration. This method can identify the variables β and γ without assuming the relationship between γ and T. Equations 9 and 10 are constraints that prevent irrational convergence values. The iterative calculations to obtain the convergent solution in the step (3) above were performed using the solver built into Excel.

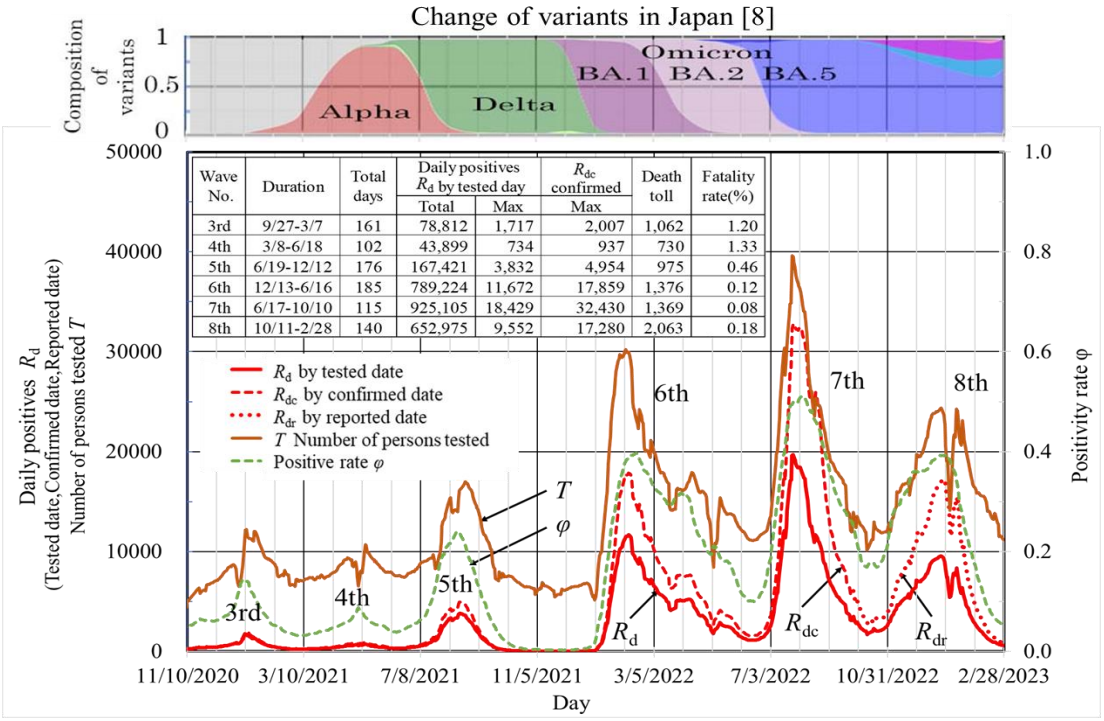

Wave No.	Duration	Total days	Daily positives R_d by tested day Total	Daily positives R_d by tested day Max	R_{dc} confirmed Max	Death toll	Fatality rate(%)
3rd	9/27-3/7	161	78,812	1,717	2,007	1,062	1.20
4th	3/8-6/18	102	43,899	734	937	730	1.33
5th	6/19-12/12	176	167,421	3,832	4,954	975	0.46
6th	12/13-6/16	185	789,224	11,672	17,859	1,376	0.12
7th	6/17-10/10	115	925,105	18,429	32,430	1,369	0.08
8th	10/11-2/28	140	652,975	9,552	17,280	2,063	0.18

Figure 1. New coronavirus COVID-19 infection status in Tokyo

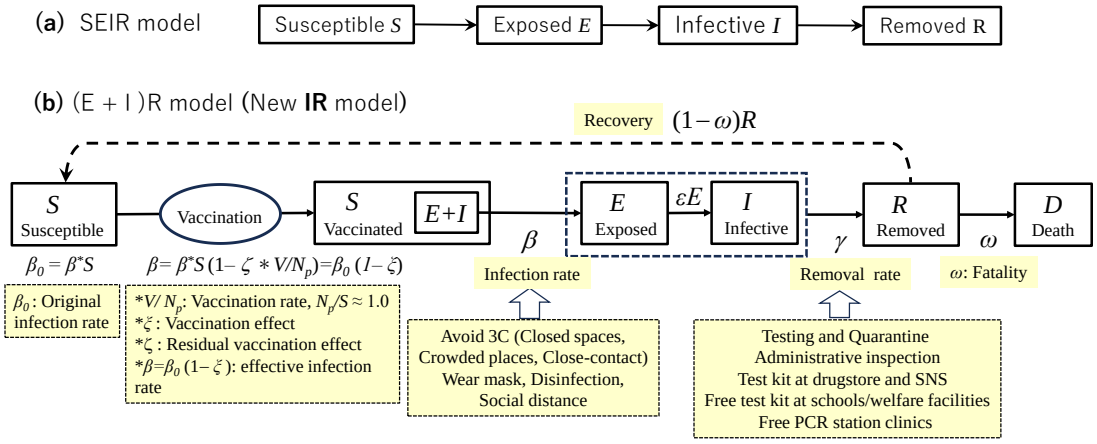

Figure 2. Diagram showing how infected persons $E+I$ in susceptible people S are infected with infection rate β, then removed to R in the healthcare system with removal rate γ. $R - D = R(1-\omega)$ can be recovered to S by the start of the next wave.

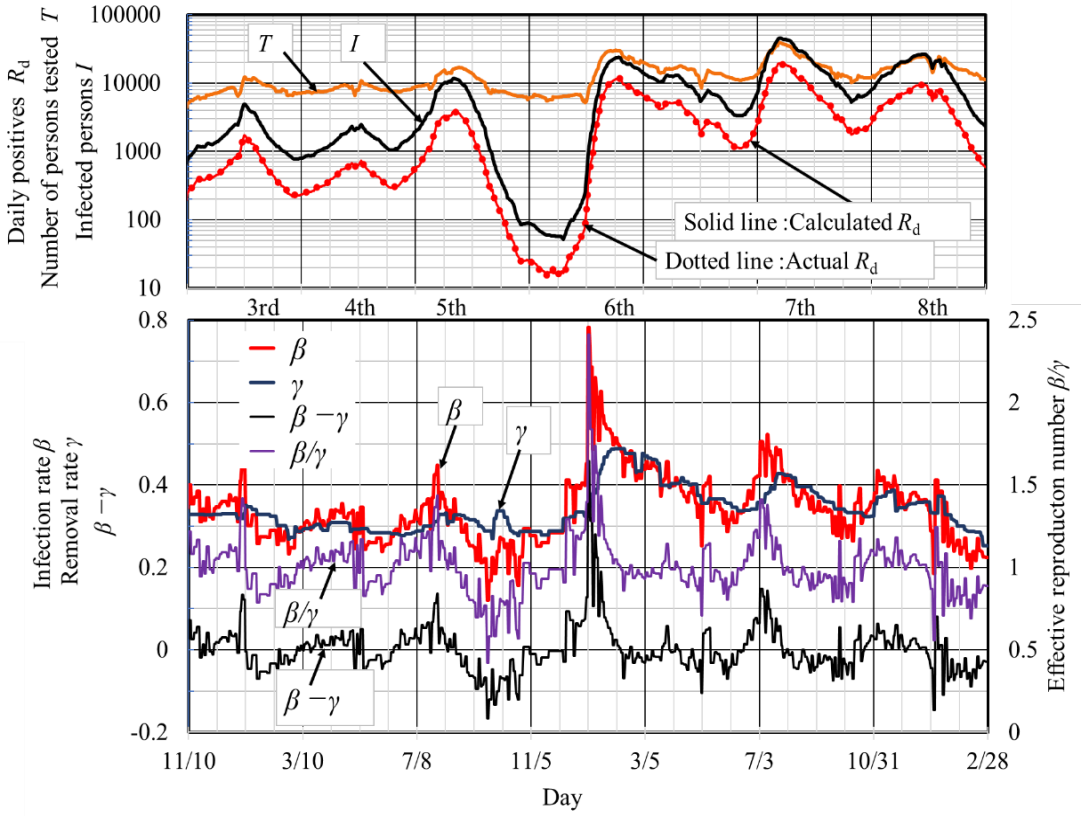

Figure 3. Identification of infection rate β and removal rate γ

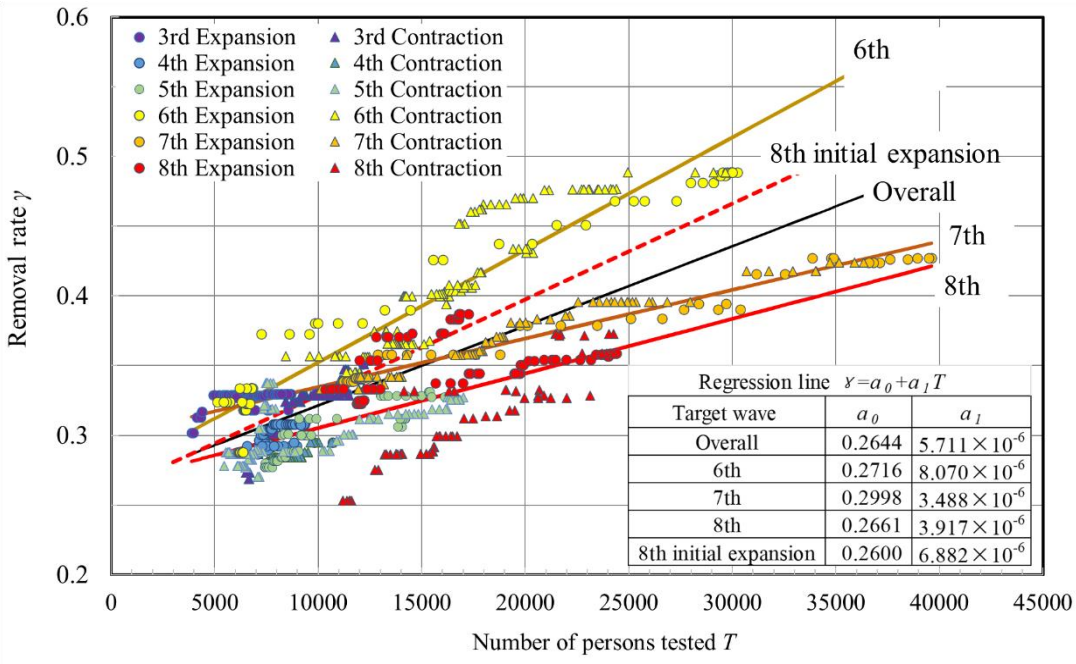

Figure 4. Relationship between removal rate γ and the number of persons tested T

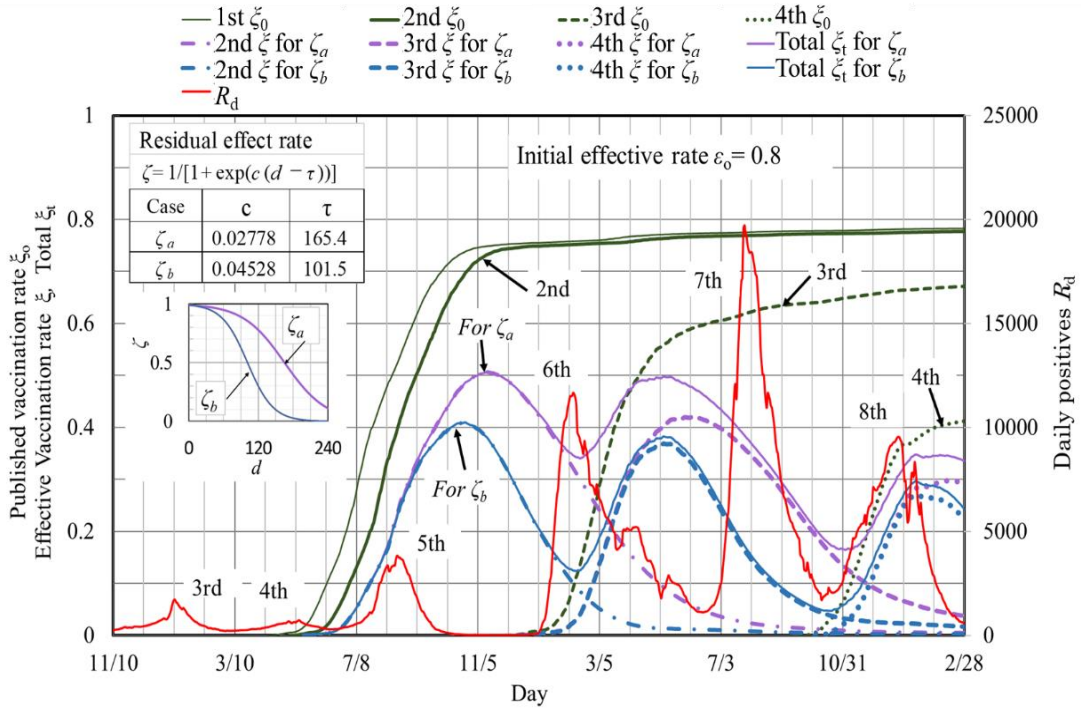

Figure 5. Effective vaccination rate and its effect on the spread of infection

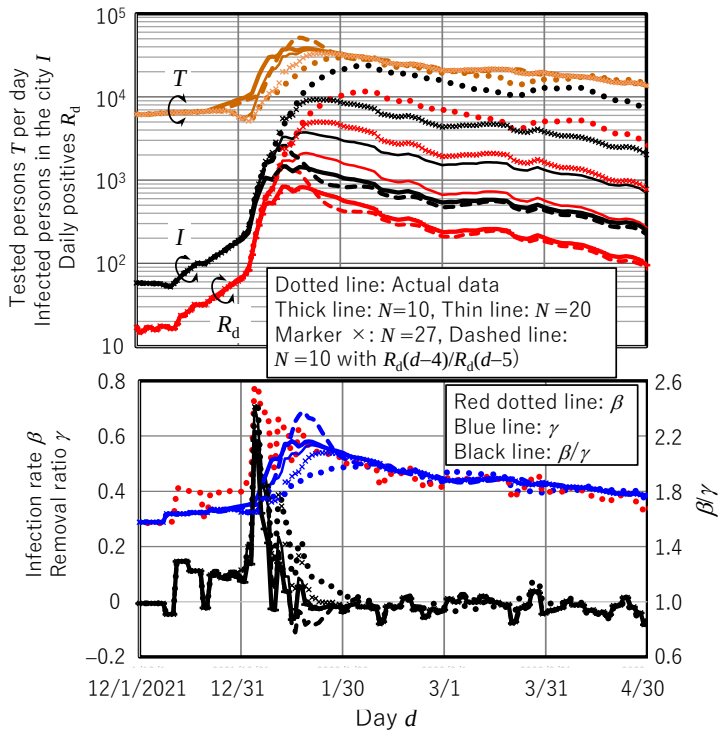

Figure 6. Simulation results of T control applied to the 6th wave when α = 0.5

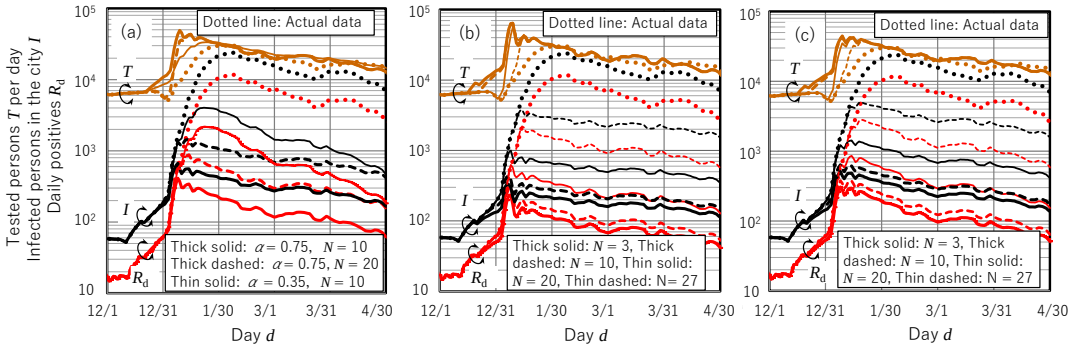

Figure 7. Simulation results of T control applied to the 6th wave. (a) T control with Equation 19 when α = 0.75 and 0.3, (b) T control with Equation 19 when α = 1.0, and (c) T control with Equation 21 when α = 1.0

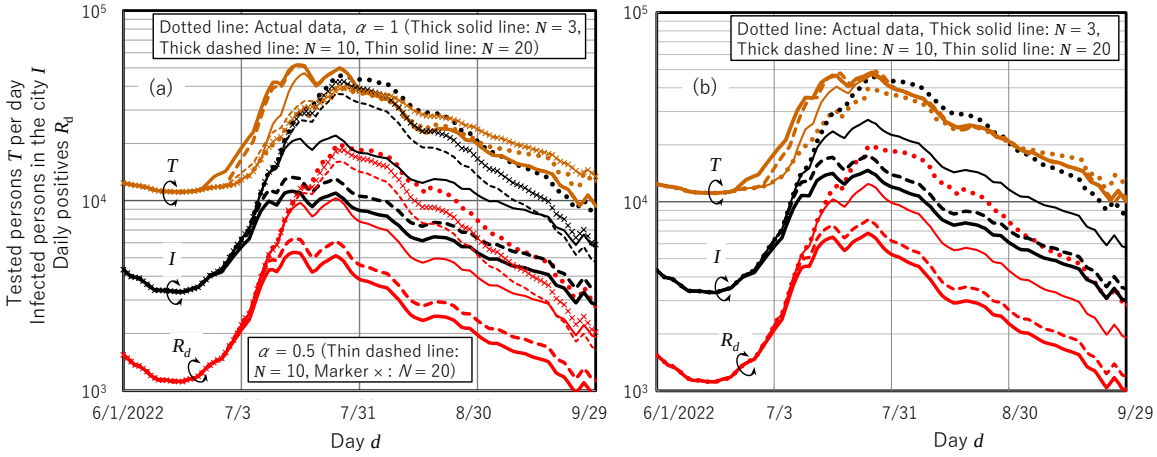

Figure 8. Simulation results of T control for the 7th wave. (a) T control with Equation 19 when α = 1 (N = 3, 10, and 20) and 0.5 (N = 10 and 20). (b) T control with Equation 21 when α = 1 (N = 3, 10, and 20)

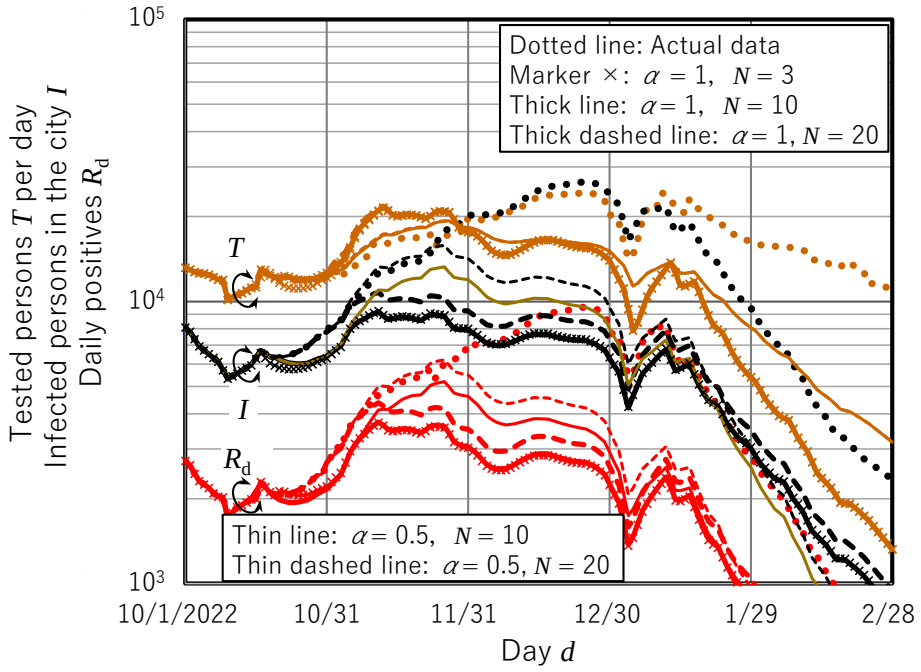

Figure 9. Simulation results of T control for the 8th wave with Equation 19 when using the relationship of $\gamma = 0.2600 + 6.882\times10^{-6}\ T$ in the early expanding period

Table 1. Comparison between $\beta_0\xi_t$ for ζ_a and γ

wave	5					6					
day	8/7	9/6	10/6	11/5	12/5	1/2	1/4	1/9	2/3	3/5	4/4
$\beta_0\xi_t$	0.069	0.128	0.211	0.28	0.277	0.342	0.580	0.345	0.279	0.268	0.357
γ	0.331	0.315	0.338	0.287	0.288	0.324	0.324	0.380	0.489	0.470	0.403
wave			7				8				
day	5/4	6/3	7/3	8/2	9/1	10/1	10/31	11/30	12/30	1/29	2/28
$\beta_0\xi_t$	0.247	0.289	0.323	0.249	0.141	0.082	0.071	0.103	0.139	0.140	0.123
γ	0.357	0.357	0.358	0.424	0.381	0.337	0.325	0.345	0.333	0.299	0.253

Analysis of effective vaccination rate

The TMG has continued to publish the daily number of persons vaccinated, the cumulative number of persons vaccinated, and the vaccination rate (cumulative number of persons vaccinated/total population, which is referred to as the published vaccination rate ξ_0 for each vaccination). It is known that not all persons vaccinated are 100% effective in preventing infection, and that a certain effective rate of infection prevention is achieved in the first several months after vaccination, and that the effective rate of infection prevention decreases over time (17,18).

Therefore, the effect of the number of persons vaccinated on reducing the infection rate in a susceptible population S is calculated by taking into account the number of people vaccinated, the effectiveness at the initial vaccination period, and the residual effectiveness rate thereafter. For this purpose, the number of persons who can be considered as having a zero equivalent infection rate is derived from the effective vaccination rate and the number of persons vaccinated, and this is defined as the effective number of persons vaccinated V. The infection rate of the susceptible population S due to vaccination is $\beta_0(1-V/S)$, where V/S is almost equal to the effective vaccination rate V/N_p, which is the ratio of the effective number of persons vaccinated V who can be considered as having a zero infectivity to the total population N_p.

The cumulative number $V(d)$ of persons effectively vaccinated on day d in a given vaccination is calculated as follows. The number of persons vaccinated on day d (the published number of persons vaccinated per day) is denoted by $W_d(d)$, the initial effective rate is ε_0, and the rate of loss of effectiveness over time is expressed as the residual effective rate $\zeta(d)$. At the start of the vaccination, day $d = 0$, the effectively vaccinated individuals are represented by $V(0) = \varepsilon_0\zeta(0)W_d(0)$. On day d after vaccination, the effective vaccinated individuals on the first day change to $\varepsilon_0\zeta(d)W_d(0)$, reduced by the residual effect of $\zeta(d)$. Similarly, the effective vaccinated persons $\varepsilon_0\zeta(0)W_d(i)$ among the persons vaccinated on day i is reduced to $\varepsilon_0\zeta(d\text{-}i)W_d(i)$ on day d. Therefore, the total effective vaccinated persons $V(d)$ is determined as the sum of all effective vaccinated persons from the first day of vaccination to day d, as follows.

$$V(d) = \varepsilon_0 \sum_{i=0}^{d} \zeta(d-i) W_d(i) \quad \text{Equation 11}$$

The effective vaccination rate for the total population N_p is given by the following equation.

$$\xi(d) = V(d)/N_p \quad \text{Equation 12}$$

Once the effective vaccinated persons in the jth vaccination are determined as $V_j(d)$, the total effective vaccinated persons $V_t(d)$ is assumed to be given by the sum of the effective vaccinated persons up to the number of vaccinations m. Thus, we have the following equation:

$$V_t(d) = \sum_{j=1}^{m} V_j(d) \quad \text{Equation 13}$$

The total effective vaccination rate for the whole population N_p is given by:

$$\xi_t(d) = V_t(d)/N_p \quad \text{Equation 14}$$

The residual effectiveness $\zeta(d)$ over time is expressed using the following sigmoid function.

$$\zeta(d) = 1/[1 + \exp(c(d-\tau))] \quad \text{Equation 15}$$

Control method for the number of persons tested T using the number of daily positives R_d

We next consider how to increase the number of T to increase the removal rate γ, especially in the early stages of an epidemic, from the point of view that strengthening the testing system in the early stages of the infection spread is the key to controlling coronavirus infection. As R_d is the only quantity to be measured, we consider using the most recent ratio $R_d(d-1)/R_d(d-2)$ for T control. The ratio of $R_d(d-1)/R_d(d-2)$ is written as:

$$R_d(d-1)/R_d(d-2) = (\gamma_{d-1}/\gamma_{d-2})\{I(d-1)/I(d-2)\} \approx (\gamma_{d-1}/\gamma_{d-2})(1 + \beta_{d-1} - \gamma_{d-1})$$

Equation 16

The variables d for β and γ are shown here in a simplified form with subscripts. If we assume that T are given by:

$$T(d) = [R_d(d-1)/R_d(d-2)]T(d-1) = (\gamma_{d-1}/\gamma_{d-2})(1 + \beta_{d-1} - \gamma_{d-1})T(d-1)$$

Equation 17

T would increase by the ratio of the 1-day prior increase in I, $1 + \beta_{d\text{-}1} - \gamma_{d\text{-}1}$, multiplied by the ratio of the 1-day prior removal rate. In principle, T must be increased in proportion to $I(d-1)/I(d-2)$ as follows:

$$T(d) = (1 + \beta_{d-1} - \gamma_{d-1})T(d-1) \quad \text{Equation 18}$$

Therefore, if we assume that:

$$T(d) = \{1 + \alpha(R_d(d-1)/R_d(d-2) - 1)\}T(d-1)$$

Equation 19,

then equation 19 coincides with equation 17 when $\alpha = 1$. Furthermore , when $\gamma_{d\text{-}1}/\gamma_{d\text{-}2} = 1$, equation 19 equal to equation 18. Because $\gamma_{d\text{-}1}/\gamma_{d\text{-}2}$ can be expressed as $1 + \delta_{d\text{-}1}$, applying this to equation 16 and substituting it into equation 19, we obtain:

$$T(d) = [1 + \alpha(\delta_{d-1} + \beta_{d-1} - \gamma_{d-1})]T(d-1)$$

Equation 20,

where δ_{d-1} can be considered as the same level as $\beta_{d-1} - \gamma_{d-1}$. If $\alpha = 1$, this would lead to an overestimation of the increase in $T(d)/T(d-1)$ during periods of expansion and an excessive decrease in $T(d)/T(d-1)$ during periods of decline, compared to equation 18. In practice, the choice of $\alpha = \sim 0.5$ is considered appropriate when δ is comparable to $\beta - \gamma$. However, when $\gamma_{d-1}/\gamma_{d-2}$ is close to 1 as in the case of slow expansion and contraction, we can use $\alpha = 1$ and equation 20 becomes closer to equation 18. Above mentioned T control based on equation 19 was applied to the 6th, 7th, and 8th waves to clarify the suppression effect on the spread of infection.

Results

Infection rate β, the removal rate γ, and effective reproduction number

Figure 3 shows the calculated results of β and γ for each R_d shown in Figure 1. The number of days in the interval is usually several days, but the minimum is two days, and the identified β and γ are shown as a series of fine step changes. The logarithmic plot in the upper part of Figure 3 shows not only the actual data of T and R_d, but also R_d and I calculated by equations 5 and 6 using the identified β and γ. We note that the calculated R_d is in excellent agreement with the actual value R_d. The calculated number of infected persons I varies almost similarly to the R_d.

The general trend is that β is between 0.2 and 0.4 and γ is around 0.3 in waves 3 to 5, whereas β is between 0.3 and 0.8 and γ is between 0.3 and 0.5 in waves 6 to 8, indicating a general increase. This may be the result of a shift from the alpha and delta strains up to wave 5, and further on to the more infectious omicron strain in waves 6 to 8. When the R_d of each wave reaches its maximum, γ reaches its maximum with the same value of β and $\beta/\gamma = 1$ holds. The β reaches its maximum at the time when the rate of increase of R_d reaches its maximum. This is due to the properties of the infection model, where infected individuals I are generated by β, and R_d is isolated by γ. After the 5th wave contraction, $\beta = 0.285$ and $\gamma = 0.288$ on 12/1/2021, while β reaches its maximum value of 0.781 on 1/4/2021 when R_d increases most rapidly. On the other hand, γ reaches its maximum value of $\gamma = 0.489$ on 2/7/2022, when R_d reaches its maximum value. The 6th wave shows a very peculiar change compared to the other waves, with a rapid increase and decrease of β.

The change in $\beta - \gamma$ is very similar to the behavior of β, with a sharp increase to 0.457 in the 6th wave on 1/4/2022. $\beta - \gamma$ corresponds to the slope of the logarithm of R_d, and the slope is steepest around this date. The change in the effective reproduction number β/γ also follows a similar trend to that of $\beta - \gamma$. The maximum value in the 5th wave is $\beta/\gamma = 1.43$, and the maximum value in the 6th wave is $\beta/\gamma = 2.41$, 1.68 times that of the 5th wave. This is consistent with the prevailing reports that the infectivity of omicron strains is 1.5 to 2 times that of delta strains. This may indicate that the stronger omicron infectivity is one of the reasons for the rapid increase in the number of β in the 6th wave.

The changes in β and γ in waves 7 and 8 are similar to those in wave 6, except for the sharp increase in β, which is progressively smaller. During the expansion period, β is larger in the 6th wave than in the 7th wave, but the maximum value of R_d is larger in the 7th wave than in the 6th wave. This is due to the value of R_d at the beginning of the expansion, which was 57 in wave 6 and 1,116 in wave 7, 40 days before the day of the R_d maximum. The fact that the 7th wave occurred before the 6th wave had sufficiently declined could be the reason why the 7th wave produced the highest number of positives. This is due to the appearance of the omicron-derived strain of BA.5 as seen in Figure 1.

Relationship between the removal rate γ and the number of persons tested T

Figure 4 shows γ determined in the previous sections separately for the expansion and contraction periods for each wave, as a function of T. Although the overall results are uneven, γ tends to increase as T increases. For each wave, γ shows a clear linear change with respect to T. Therefore, regression lines were plotted for all waves from wave 3 to 8, wave 6 only, wave 7 only, and wave 8 only. The resulting regression line equations are shown in the figure.

The resulting regression line equation for the wave 6 (yellow line) is clearly in the upper zone, while wave 7 (brown line) is in the lower zone, and wave 8 (red line) is in the lowest zone, compared to the regression line for the whole wave (black line). In the 7th wave, both γ in the expansion period and γ in the contraction period show little variation from the regression line, and the proportionality of γ to T is evident. In contrast, the 8th wave shows separate trends in the early expansion (10/11/2022 to 11/22/2022), mid-expansion (11/23/2022 to 1/15/2023), and contraction (1/16/2023 to 2/28/2023) periods. For the simulations, a regression line for the early expansion period is also shown in Figure 4.

Impact of effective vaccination rate

The effectiveness of vaccines has been analyzed and evaluated by the WHO and other organizations, and the initial effectiveness and duration of the vaccine have been published . Effectiveness varies considerably depending on the type of vaccine, the type of coronavirus, and the age groups vaccinated. Initial efficacy rates range from the upper 90% to the lower 40%. The effective rate is said to maintain the initial effectiveness for several months, but the effectiveness declines significantly after 5 or 6 months (17,18). In this paper, with reference to the literature (17,18) and other sources, we assume the following conditions for the effectiveness of mRNA vaccination in Tokyo: 1) The effect occurs 2 weeks after vaccination, 2) The initial effective rate is $\varepsilon_0 = 0.8$, 3) The residual effective rate ζ is defined as: a) ζ_a: The ζ changes from 0.99 on the first day to 0.4 after 180 days (the effective rate decreases from 0.8 in the initial period to 0.32 after six months.), and b) ζ_b: The ζ changes from 0.99 on the first day to 0.1 after 150 days (the effective rate decreases significantly from 0.8 in the initial period to 0.08 after 150 days).

The results of the effective vaccination rate calculated from the Corona vaccination data in Tokyo are shown in Figure 5. Figure 5 shows R_d, ξ_0 from the first to the fourth vaccination, and ξ and ξ_t for each vaccination and for the total vaccination . The first vaccination started on 4/21/2021, followed by the second vaccination 12 days later on 5/3/2021. As almost all the persons were re-vaccinated within a few weeks, the effective vaccination rate was calculated from the second vaccination. The residual effective rates ζ_a and ζ_b and their parameter values of c and τ are shown in Figure 5. The effective vaccination rate ξ for each of the second, third, and fourth vaccinations starts to increase two weeks after the corresponding published vaccination rate ξ_0 , reaches a maximum value after 4~5 months, and then decreases after 6~8 months. The difference in the characteristics of the effective residuals is that the ζ_b case loses its effectiveness 2~3 months earlier than the ζ_a case , and the maximum effective vaccination rate is also more than 0.1 smaller than that of the ζ_a case. The maximum value of ξ for each vaccination is much smaller than the published vaccination rate ξ_0 for the corresponding vaccination.

Under the condition of the residual effective vaccination rate ζ_a for the second vaccination , the maximum value of the ξ is 0.507 on 11/14/2021, which is 66% of the corresponding the value of the published vaccination rate of 0.733. The total effective vaccination rate ξ_t, which is the sum of the results of each vaccination , reaches a maximum near the maximum value of the ξ for each vaccination and a minimum near the beginning of the third and fourth vaccination.

The total effective vaccination rate ξ_t shows the effect of vaccination on each wave. In the 5th wave, R_d decreases as ξ_t increases, and when the ξ_t reaches its maximum , the R_d remains at the lowest level of around 20. As the ξ_t decreases, the 6th wave begins to increase rapidly and reaches its maximum peak when the ξ_t is at its minimum . The minimum value of ξ_t is 0.34 for the case of residual effect ζ_a, but is much smaller at 0.12 for the case of ζ_b. The magnitude of the effect on the suppression of the 6th wave expansion was small for ζ_b. It can be said that the start of the third vaccination was delayed even though the effect of the second vaccination had decreased significantly . The β shown in Figure 3 is the value when the vaccination effect is at work. If the infection rate in the absence of the vaccination effect is defined as β_0, it is given by $\beta_0 = \beta/(1-\xi_t)$. Therefore, the rate of decrease of β relative to β_0 is $\xi_t = (\beta_0-\beta)/\beta_0$. Because ξ_t is 0.205 (for ζ_b) and 0.426 (for ζ_a) when β reaches its maximum (0.781) in wave 6, the maximum value of β_0 would have temporarily reached 0.983 and 1.36 (cluster infection), respectively. When R_d is at its maximum, β is 0.493 and $\beta/\gamma = 1$, and the reduction effect ξ_t for β and β/γ due to vaccination is 0.125 (for ζ_b) and 0. 346 (for ζ_a).

After the third vaccination , the effective rate starts to increase again. ξ_t reaches its maximum around the time between the 6th and 7th wave, suggesting that the total effect of the second and third vaccinations contributes to the reduction of β by 0.37 (for ζ_b) and 0.5 (for ζ_a).

The 7th wave increases as ξ_t begins to decrease and reaches its largest peak when ξ_t is around 0.2 (for ζ_b) to 0.4 (for ζ_a). When β is at its maximum (0.523), the rate of decrease ξ_t in β relative to β_0 is 0.191 (for ζ_b) and 0.398 (for ζ_a). When R_d is at its maximum, β is 0.425, $\beta/\gamma = 1$, and ξ_t is 0.153 (for ζ_b) and 0.369 (for ζ_a). Therefore , if the actual vaccine effectiveness was close to ζ_a, it can be said that the vaccination played an important role in reducing the infection rate from the beginning to the peak of wave 7.

However, from the assessment (17) that the vaccine effect was lower for strain BA.5 in wave 7 than for strain BA.1 in wave 6, it is likely that the residual effect rate ζ_b reflects the real situation. Although the ξ_t continued to decline, the R_d decreased thereafter in wave 7. It is thought that vaccination did not have much effect during the contraction period of wave 7, and that factors such as the expansion of the inspection system were more effective.

The 8th wave began when ξ_t was close to a minimum level. By the time R_d had risen to a maximum, ξ_t had almost caught up with the increase in R_d due to the fourth booster vaccination. It is then likely that wave 8 decreased due to the higher value of ξ_t. When R_d is at its maximum, β is 0.365 and $\beta/\gamma = 1$, and ξ_t is 0.253 (for ζ_b) and 0.308 (for ζ_a). Although, the published vaccination rate ξ_0 for the fourth vaccination is low, at only 0.4, the ξ_t is in the range of 0.3 to 0.4, and the vaccination effect in wave 8 is comparable to the cases in waves 6 and 7.

Impact of *T* control in suppressing epidemic waves

Suppressive effect of T control on the 6th wave of infection

First, for the 6th wave, in which the effective reproduction number β/γ increased to 2.4, we calculated how much suppression of infection is achieved when the number of persons tested is controlled, based on
$T(d) = \{1 + \alpha[R_d(d-1)/R_d(d-2) - 1]\}\, T(d-1)$ during the period of infection spread . In the simulation , γ was first calculated using the equation $\gamma = 0.2716 + 8.070 \times 10^{-6} T$, which is the average relationship between γ and T in the 6th wave identified in Figure 4. $I(d) = \exp(\beta_d - \gamma_d) I(d-1)$ was then calculated using the γ and the infection rate β_d. Daily positives $R_d(d) = \gamma_d I(d)$ was then calculated . The start of T control was changed from the start of spread when the actual daily positives $R_d(d+1)/R_d(d) \geq 1$ occurred on three consecutive days. $d+1$ was defined as the start of spread and $N =$ 3, 10, 20 and 27 days thereafter were chosen as the start dates of T control. The start date of the 6th wave of infection spread was 12/13/2021.
Figure 6 shows the number of persons tested T, the number of persons infected in the city I and the number of daily positives R_d for each test day in brown, black and red, respectively, for the case $\alpha =$ 0.5 with N = 10 (d = 12/23/2021), 20 (d = 1/2/2022) and 27 (d = 1/9) as control start dates. The infection rate β, the removal rate γ and the effective reproduction number β/γ are shown in red, blue and black respectively in the lower part of the figure. In Figure 6, the thick dotted lines indicate the actual values of T, R_d and the calculated values of I, β, γ and β/γ. The simulation results with T control are shown as thick solid, thin solid and marker × for N = 10, 20 and 27 respectively. The thick dashed line shows the case where $T(d) = \{1+0.5[R_d(d-4)/R_d(d-5) - 1]\}\, T(d-1)$ using the R_d values from four and five days ago in equation 19. From this, the following can be said:

1) The actual maximum value of R_d is 11672 persons on 2/7, but the maximum value of R_d in the T control is 836 on 1/14 when N = 10, 2094 on 1/19 when N = 20 and 4991 persons on 1/23 when N = 27. The maximum value of R_d is reduced to 7, 18 and 43% of the actual value. Furthermore, the day of maximum R_d is 24, 19 and 15 days earlier for N = 10, 20 and 27 respectively. The maximum value of $R_d(d)/R_d(d-7)$ was 10.3 on 1/8 day of N = 26. Therefore, if the T control had been initiated on that day, the maximum value of R_d would have been 1/2 of the actual value 15 days earlier. For N = 10, if $R_d(d-4)/R_d(d-5)$ and the data from four days ago are used for T control, the overshoot phenomenon occurs with a time lag in the increase of T, R_d, and I. It is therefore important to use the most recent rate of increase of R_d for T control.

2) T control according to equation 19 was performed during the contraction period of R_d after the start date N. As shown in the upper part of Figure 6, after R_d reaches its maximum value, it is reduced almost in parallel with the reduction characteristic of R_d in the actual case. During the contraction period, T can be reduced by T control, but the controlled T value is almost the same as the actual T, except for some periods. However, it is not clear why the controlled T value stagnates at around 20,000 persons from 3/1 to around 3/31, and the controlled R_d and I also show the same trend . The characteristics of the 6th wave $\gamma = f(T)$ shown in Figure 4 probably cannot be represented by a single regression line , and the difference between the regression line used and the actual values is likely to have an effect . The β and β/γ in the lower part of Figure 6 also deviate from the actual values during this period.

3) The lower part of Figure 6 shows that the removal rate γ can increase and cross the line of β corresponding to the time when R_d reaches a maximum and β/γ decrease to 1, as quickly as N decreases. Although the transient behavior of β/γ is not clear around day 1/4, the maximum value of β/γ is reduced to 2.14 at N = 10 but does not change in other cases.

4) The simulation shown in Figure 6 uses the actual value of β. However, in the actual T control, β is also changed to be lower than the actual value due to the T control. Therefore, the result in Fig. 6 is the worst case, and R_d and I are considered to shrink faster in reality than the results in Figure 6.
Next, the variation of the T control characteristics with varying α is shown in Figures 7(a) and 7(b). Figure 7(a) shows the changes in T, I and R_d due to T control for α = 0.75 with N = 10 and 20, and for α = 0.35 with N = 10. For α = 0.75 and N = 10, the suppression effect of the T control is greater than for

α = 0.5 and N = 10 in Figure 6. During the start-up process, R_d reaches a maximum value of 412 on 1/8 day, which is reduced to 3.5% of the actual maximum value of R_d of 11672. However, the small transient oscillation occurs in the control value of T, which then induces the small similar variations in R_d and I. This phenomenon will be caused by the overestimation of the control coefficients due to the removal rate γ and the time delay of the control coefficients. On the other hand, for N = 20, R_d reaches a maximum value of 879 persons on 1/14 day, which is 7.5% of the actual value and therefore almost the same as for N = 10 with α = 0.5. However, the decrease in R_d after two months is 1.5 to 2 times greater for α = 0.5 and N = 10. In the case of α = 0.35, N = 10, R_d reaches its maximum value of 2175 persons on day 1/22, after which it decreases more rapidly than in the case of α = 0.75. The maximum value of R_d is therefore 19% of the actual value 16 days earlier than the actual value. From Figure 7(a), α = 0.75 is considered preferable for T control because the variation of T is small enough to be allowed. The earlier the control starts, the better. However, in practice it may not be easy to increase T as calculated, so this theoretical value can be considered as a target for the desired number of persons T to be tested.

Figure 7(b) shows the simulation results for N = 3, 10, 20 and 27 when α = 1. When α = 1, not only R_d and I, but also the control variable T, experience strong overshoot oscillations after the start of the control for N = 3, 10, 20 which is not practical. The reason for this is that the control coefficient is amplified by the factor $\gamma(d-1)/\gamma(d-2)$ during the high infection expansion phase, resulting in the transient oscillations in the second order system. Because the relationship between T and γ in the 6th wave was known, the T control was carried out using the following equation for α = 1, cancelling the effect of $\gamma(d\text{-}1)/\gamma(d\text{-}2)$:

$$T(d) = \left\{\frac{R_d(d-1)}{R_d(d-2)}\right\}\left\{\frac{\gamma(d-2)}{\gamma(d-1)}\right\}T(d-1)$$

Equation 21

Figure 7(c) shows the simulation results for N = 10, 20 and 27. Compared to Figure 7(b), the violent oscillation amplitudes of T are significantly suppressed; R_d and I still have small oscillations. The control law in equation 21 cannot be used because the relationship between γ and T is unknown. Therefore, it is considered advisable to use equation 19 with α = 0.5~0.75 as the T control target and to set up a control system.

Suppressive effect of T control on the 7th wave of infection

Next, we describe the simulation results when the T control is applied to the 7th wave, which caused the largest number of COVID-19 cases in Tokyo. For the simulation of the 7th wave, the regression equation $\gamma = 0.2998+3.488\times10^{-6}T$ of the relationship between γ and T in the 7th wave shown in Figure 4 was used. First, the results of the T control are shown in Figure 8(a) when α = 1 and N = 3, 10 and 20 from the beginning of the expansion, and when α = 0.5 and N = 10 and 20. The actual values of T and R_d for the 7th wave and the estimated infected persons in the city I are shown as brown, red, and black dotted lines, respectively. The minimum R_d value between the 6th and 7th wave is 1116 on 6/16 and the start of the continuous rise is on 6/17. The R_d reached a record high of 19720 on 7/26.

In contrast, the R_d of the T control with α = 1 and N = 10, shown by the thick dashed red line, reaches its maximum value of 6291 on 7/15, i.e., 11 days earlier than the actual date, and falls to 32% of the actual R_d maximum value. It then falls again, but reaches a second peak of 6118 on 7/25 close to the date of the actual R_d maximum. This may be due to the fact that the actual value of R_d reaches a local maximum on 7/15, then a local minimum of 11360 on 7/17, and continues to rise. Synchronously with the actual value of R_d, the controlled value T also increases after maxima and minima, and the controlled values of R_d and I are thought to follow the same pattern.

The control result of R_d after the second maximum on 7/25 shows a slightly slower decrease than the actual value of R_d, which may be due to the control value of T decreasing slightly faster than the actual T value. The control result for N = 3 is shown as a thick solid line for reference. In this case the maximum value of R_d is only 84% lower than for N = 10. The control results for α = 1 and N = 20, shown by the thin solid line, show a first maximum R_d of 9734 on 7/16, which is 49% of the actual maximum, and a second maximum of 10316 persons on 7/26, which is 52% of the actual maximum. The T control values for N = 3 and 10 overlap after the first maximum of R_d on 7/16.

Next, looking at the case where α = 0.5, R_d has a maximum value of 16034 on 7/26 when N = 10, which is only 81% of the actual value. The subsequent rate of decrease of R_d is slightly faster than the actual value probably because the number of T increases slightly more than the actual value. In the case of N = 20, there is almost no effect of the T control on the reduction of R_d. From these results it can be said that in the 7th wave, the maximum value of R_d can be suppressed to less than 1/3 of the actual

value if T control is performed at α = 1 and N = 10 or less.

Incidentally, Figure 8(b) shows the simulation results when T control based on equation 21 is started at N = 3, 10 and 20. Compared to the case with α = 1 in Figure 8(a), the degree of reduction in the maximum value of R_d is about 40% for N = 10, but the required number of T also decreases consistently.

The above results indicate that in the 7th wave, the reduction effect of R_d by T control is significantly smaller than in the 6th wave. The reason for this is probably that the test system in TMG was significantly strengthened compared to that in the 6th wave.

In fact, the TMG has announced in its "TMG Inspection System Improvement Plan for New Coronavirus Infections (Revised on April 28 2022)" that, based on the maximum number of cases tested at the peak of the 6th wave, which was the largest ever, a total of approximately 290,000/day is secured (a maximum of approximately 100,000 cases/day for administrative testing, a maximum of about 40,000 cases/day for distribution of antigen kits to close contacts, a maximum of 100,000 cases/day for TMG own testing and a maximum of about 100,000 cases/day for distribution of antigen kits to close contacts).

In addition, to strengthen the inspection system from April, the following measures were taken:

1) a smooth consultation system by announcing of all medical institutions for examination and treatment;
2) strengthening the capacity of medical institutions and private inspection institutions to analyze tests (equipment assistance);
3) encouraging an increase in the number of facilities subject to intensive testing and the frequency of implementation; and
4) using the continued involvement of staff who have become concentrated contacts in institutions subject to intensive testing for testing (19).

On August 17, the Ministry of Health, Labor and Welfare announced that to overcome the shortage of medical treatment and testing facilities (fever outpatient clinics), antigen test kits would be made available as over-the-counter (OTC) drugs, and citizens would be able to obtain and test them individually at drugstores and on the Internet, with positive results reported to the registration center and others for health monitoring guidance (20). In view of the strained medical situation of the 7th wave, Japan was finally able to obtain antigen test kits at a level like that in Europe and the USA.

Suppressive effect of T control on the 8th wave of infection

Finally, we describe the simulation results when T control is applied to the 8th wave, in which the maximum value of R_d was 9552 on 12/25/2021. As shown in Figure 4, the 8th wave shows different characteristics of the removal rate γ with respect to T in the early, middle and reduction periods, possibly due to the occurrence of omicron-derived species. First, calculations using the averaged regression line equation $\gamma = 0.2661 + 3.917\times10^{-6}T$ throughout the expansion and contraction periods showed inappropriate characteristics. Then, the regression characteristic $\gamma = 0.2600 + 6.882\times10^{-6}T$ in the early expansion period was used for the T control simulation, and reasonable results were obtained, as shown in Figure 9.

It has been shown by the red dotted line in Figure 9, the actual value of R_d between waves 7 and 8 reached a minimum of 1706 persons on 10/10/2022 and increased for three consecutive days from 10/11, so 10/11 was defined as the zero date for the start of the expansion. The simulation results for T, I and R_d under T control with α = 1 after N = 3 (10/14), 10 (10/21) and 20 (10/31) days from the expansion start date are shown with a marker ×, a thick solid line and a thick dashed line, respectively. The results of T, I and R_d when the T control was performed at N = 10 and 20 days with α = 0.5 are shown as thin solid and dashed lines, respectively. The actual value of R_d has a small maximum on 10/17, followed by a minimum on 10/21, and then increases almost monotonically to a maximum of 9552 on 12/25 and a second maximum of 8337 on 1/10/2023.

First, we focus on the results of the T control for α = 1 and N = 10, because the T, I and R_d for α = 1 and N = 3 marked with × coincide in most regions with the T, I and R_d for α = 1 and N = 10 shown by the thick solid line. R_d shows a first maximum of 3720 on 11/11 and a second maximum of 3607 on 11/23; thus, the second maximum due to the T control shows a maximum of 38% of the actual value 30 days earlier and then decreases by about 2/5 of the actual value. For N = 20, R_d shows a maximum of 4379 on 11/11 and a maximum of 4206 on 11/23, with the second maximum decreasing to 44% of the actual maximum 32 days earlier, and then decreasing at the same rate as for N = 10. On the other hand, the number of T for N = 3, 10 and 20 is almost the same after day 10/31. The number of T required to suppress the maximum value of R_d should be increased to about 1.4 times the actual value around 11/12 in the early expansion stage, whereas the value of T in the T control during the

contraction period after about 11/30 days is significantly smaller than the actual value. This is because the increase in R_d is suppressed by the increase in T in the early expansion phase, allowing R_d to be efficiently reduced with less T in the contraction period. Therefore, in any epidemic wave, providing the number of T calculated by the T control equation in the early stages of infection spread will allow the peak of R_d to be much earlier than the actual case and the number of T in the contraction period to be reduced.

The results for $\alpha = 0.5$ and $N = 10$ and 20 show that the T values are almost the same after 10/31. The red thin solid and dashed lines for $N = 10$ and 20 show that the maximum value of R_d is 5202 and 6211 on 11/25, 54 and 65% of the actual value, respectively. The smaller α, the smaller the increase in T and the smaller the decrease in I and R_d, so the T control with $\alpha = 1$ is suitable for the 8th wave. However, compared to the 6th wave, the reduction effect of the T control on R_d and I is much smaller. The reason for this is that, as in the 7th wave, free test kits were provided to educational, medical and welfare institutions, and citizens were in an environment where they could obtain test kits as needed.

In Figure 9, when $\alpha = 0.5$ and $N = 20$, the calculated I and R_d during the infection spread period are slightly larger than their actual values, which is inconsistent result. The reason for this is that the average relationship between γ and T during the spread period used in the T control law differs from the actual characteristics in this region, as can be estimated from Figure 4. The similar simulation results were obtained when the averaged regression line equation $\gamma = 0.2661 + 3.917\times10^{-6}T$ was used. The T control by equation 19 automatically acts on the relationship between γ and T in real time, so this problem cannot occur.

The above results show that even when the test system is well established, the T control with $\alpha = 1$ can suppress the maximum value of R_d to about 40% of the actual value one month before, and then change to a declining phase if the start date of the T control is within 10 days of the start date of the outbreak.

Discussion

As mentioned in the analysis of the 5th wave (5), when effective reproduction number = $\beta/\gamma = RN > 1$, the only way to reduce the RN below 1 is to restrict social activities and human flows and intensify vaccination so that the infection rate β becomes $\beta' \le \beta/RN$, or to intensify testing activities so that the removal rate γ increases to $\gamma' \ge RN \times \gamma$. During the two and a half years of the COVID-19 epidemic from 2020 to mid-2022, the medical administration in Japan and the city of Tokyo was mainly devoted to reducing β by restricting social and economic activities. The importance of policies to increase γ seems to have been overlooked. The previous paper (5) showed that the peak of the 5th wave could have been suppressed to less than half if the number of tests had not been halved during the consecutive holidays of the Olympic opening and closing events. In this paper, we find that the size of the peak in daily positives R_d is strongly determined by the daily expansion ratio of R_d in the early expansion period and propose a general method to suppress β/γ in the early expansion period by increasing the number of persons tested T in proportion to $R_d(d)/R_d(d-1)$.

In Japan, the rapid decline in R_d from mid-August to the end of September in the 5th wave, is thought to be mainly because of the vaccine. Indeed, the rapid decline in β from mid-August to mid-September in Figure 3 is thought to be due to the vaccine effect. However, it should be noted that the γ value did not decrease much during this period, and R_d decreased rapidly because $\beta-\gamma$ continued to take large negative values. Despite the large increase in β around 10/6, γ also increased in response to this, so that $R_d < 40$ was maintained from 10/21 to 12/26. Because the daily rate of increase in positives I is $\beta-\gamma$, we can compare the contribution of vaccination to the decrease in $\beta-\gamma$ with that of γ. Using the infection rate β_0 in the absence of vaccine, $\beta = \beta_0(1-\xi_t)$, so that $\beta-\gamma = \beta_0-\beta_0\xi_t-\gamma$. Therefore, the effects of vaccination and testing can be compared quantitatively using the values of $\beta_0\xi_t$ and γ. Table 1 compares the values of $\beta_0\xi_t$ and γ every 30 days from 7 Aug 2021 to 28 Feb 2023, obtained from the β and γ in Fig. 3 and ξ_t for ζ_a in Figure 5.

Table 1 shows that $\beta_0\xi_t$ is one third of γ even in the 5th wave contraction period on 9/6 and becomes two third on 10/6 and almost equal to γ on 11/5 and 12/5. Therefore, the main reason for the rapid decline of R_d in the 5th wave from mid-August to the end of September is mainly attributed to the effect of γ. The long period of suppression from October to the end of December was equally supported by the effects of vaccination and testing. The effect of $\beta_0\xi_t$ was unusually larger than γ on 1/4, but as can be seen from Figure 3, this was due to a steep increase in β. However, the effects of $\beta_0\xi_t$ and γ are comparable around dates 1/2 and 1/9. During the peak of the 6th wave, from 2/3 to 3/5, $\beta_0\xi_t$ was less than 60% of γ. During the period from 4/4 to 8/2, from the decreasing phase of the 6th wave to the peak of the 7th wave, it was increased to 60–90% of γ. This trend corresponds to the wave shape of the vaccine effect ξ_t for ζ_a in Figure 5. It can be concluded that vaccination

had a suppressive effect on infection from the period of convergence of the 5th wave to the peak of the 7th wave, which was almost as large as the γ effect. However, between 9/1 and 2/28, immediately after the peak of the 7th wave, $\beta_0\xi_t$ effect was less than 50% of the γ effect. This was due to the warning effect of the third vaccination and a marked decrease in the vaccination coverage of the fourth vaccination, which started around 31 October. As mentioned before, around high R_d values in the 7th and 8th waves, the effect of the testing system in reducing R_d was almost saturated, suggesting that the maximum value of R_d could have been suppressed by increasing the vaccination rate.

The delayed response of the testing regime in the early stages of the 6th wave expansion may have been dominated by a sense of relief from the 3-month period of reduced R_d. Indeed, following the convergence of the 5th wave, $R_d < 40$ was maintained for more than two months from 10/21/2021 ($\gamma = 0.283$) to 12/25/2021 ($\gamma = 0.334$). However, in the following week, on 1/1 ($\gamma = 0.324$), R_d increased by a factor of 1.71. However, $R_d = 66$ was in double digits, so it is unlikely that they felt very threatened. However, the next week later, on 1/8 ($\gamma = 0.373$), the R_d number increased by a factor of 9.39 to 619. This rapid increase was partly due to the high infection rate of Omicron derivatives, but also to the fact that the average number of tests during the five-day period from 12/31 to 1/4 was reduced to 82% of that in the period from 12/26 to 12/30 due to the New Year holidays. Therefore, one week later, on 1/15, $\gamma = 0.426$, and the rate of increase in R_d decreased to 4.44 times. In Figure 6, the start dates of T control for $N = 10$, 20 and 27 correspond to 12/23, 1/2 and 1/9, respectively, so it would have been difficult to start T control at $N = 10$ and 20. However, it should be noted that starting on 1/9 of $N = 27$ would have allowed the peak of R_d to be passed less than 1/2 of the actual peak value two months earlier. Therefore, it is important to start T control as early as possible to suppress the peak of the epidemic wave.

In Figure 4, the proportionality factor of γ to the number of persons tested T is higher for wave 6 than for the other waves, indicating that the efficiency of finding positive persons through testing is high. On the other hand, for waves 7 and 8, the efficiency of γ with respect to T is lower than the overall average value in the region where the number of tests T and R_d are large. However, the increase factor of γ with respect to T is higher than the average value in the early stages of the expansion, suggesting that the maximum peak of R_d can be reduced by more than half if T control is started within $N = 10$, as described in sections 3.4.2 and 3.4.3.

In the future, experts in infectious disease epidemiology and economists will need to work together to use COVID-19 data to determine the relationship between economic losses due to reduced economic activity and the rate of decrease in β, the cost of vaccine purchases and vaccination regimes and the rate of decrease in β, and the costs of testing regimes and the rate of increase in γ. It is also expected that a comprehensive assessment will be made as to how much human and economic resources can be invested in strengthening vaccination and testing activities to maximize the cost-effectiveness of suppressing infectious diseases, while limiting the loss of national economic capacity due to reduced economic and social activities. We hope that the analytical methodology of this study and its application to waves 6, 7, 8 will serve as a reference for future consideration of such comprehensive policy for the control of infectious diseases.

Conclusion

In this paper, we first formulated a simplified ***IR*** theory, in which ***I*** and ***R*** include both exposed and symptomatic, suitable for the COVID-19 epidemic analysis. The ***IR*** model was then used to analyze the epidemic situation in the 6th, 7th, and 8th waves in Tokyo. A numerical analysis method was formulated to analyze the number of infected persons in the city I, the infection rate β, the removal rate γ and the effective reproduction number β/γ from the data on the daily number of positive cases R_d. The transition of these quantities from the 3rd to the 8th wave was clarified. In wave 6, caused by the omicron variants, the infection rate and the effective reproduction number increased dramatically to 0.78 and 2.4, respectively, in the early stages of expansion, leading to an increase in R_d and a strain on the medical system due to delays in the testing system and a shortage of test kits. In waves 7 and 8, the quarantine and testing systems were significantly strengthened, but the high infectivity of the omicron-derived strains resulted in even more positive cases in wave 7. Taking into account the changes in vaccination rate over time and the effect of suppression of infection rates, we assessed the overall effect of the second, third and fourth booster vaccinations in reducing infection rates and found that the effect of reducing infection rates and effective reproduction number at the maximum of waves 6, 7 and 8 waves was 13–35, 15–37, and 25–31%, respectively. Furthermore, we also showed how the effect of vaccination on reducing infection rates can be assessed in comparison with the effect of removal rate.

Next, to restrict the spread of infection, we devised the *T* control approach, in which the number of people tested *T* is proportional to the rate of increase in R_d. We simulated the impact of applying this strategy to waves 6, 7, and 8 using the measured relationship between *T* and γ in each wave. The results revealed that in wave 6, the maximum value of R_d could be reduced to less than a tenth of the value three weeks earlier when the *T* control method was applied 10 days after the start of the expansion, and to half of the value two weeks earlier when the *T* control method was applied 27 days after the start of the expansion. In contrast, the quarantine and inspection regimes in the 7th and 8th waves were greatly intensified when compared to the 6th wave. However, if *T* control was implemented within 10 days of the start of the expansion, the maximum R_d in the 7th wave might be reduced to 1/3 of the real maximum value, and to 40% of the actual value one month before the actual maximum date in the 8th wave.

We believe that the new ***IR*** theory of infectious disease, the method for calculating the infectious population in the city, the infection rate, the removal rate, and the overall vaccination effect, as well as the *T* control method, will be a powerful tool for quantitatively evaluating the spread and contraction of the epidemic wave and future infection prevention measures. We hope that in the near future, infectious disease theorists and economists will collaborate to determine what policies will maximize society's cost-performance ratio, taking into account the loss of national expenditure and human power due to reduced socioeconomic activity and infection rates, the cost of vaccination regimes and infection rate reductions, and the cost of testing regimes and removal rate increases. We feel that this study will supply the necessary materials for this project.

References

1. WHO Covid-19 dashboard Japan Cases. Available from: https://data.who.int/dashboards/covid19/cases.
2. Kuniya, T., Inaba, H., Possible effects of mixed prevention strategy for COVID-19 epidemic: Massive testing, quarantine and social distancing. AIMS Public Health 2020; 7:490–503.
3. Shimizu, K., Kuniya, T., Tokuda, Y. Modeling population-wide testing of SARS-CoV-2 for containing COVID-19 pandemic in Okinawa, Japan. J Gen Fam Med 2021;22(4):173-181.
4. Ono, K. and Kikuchi, K. [Analysis and Suppression Measures of New Coronavirus Infection Epidemic in Tokyo, Japan] (in Japanese) JSME, August, 2020. Available from: https://www.jsme.or.jp/activity-to-covid19/20200810.
5. Ono, K., Numerical Analysis of the Fifth Wave of COVID-19 epidemic in Tokyo, Japan, Int J Epidemiol Health Sci 2022;3(3): e28.
6. WHO Covid-19 dashboard Japan Vaccines. Available from: https://data.who.int/dashboards/covid19/vaccines?m49=392&n=c.
7. [Open data on new coronavirus infections before the transition to category 5 (by May 8, 2023)] (in Japanese), Bureau of Public Health, Tokyo Metropolitan Government. Available from: https://www.hokeniryo.metro.tokyo.lg.jp/kansen/corona_portal/info/covid19_opendata.html.
8. Covariant, Overview of Variants in Countries. https://covariants.org/per-country?country=Japan.
9. Kuniya, T. Structure of epidemic models: toward further applications in economics, Jap Economic Review 2021;72:581-607. https://doi.org/10.1007/s42973-021-00094-8.
10. Kunuya, T. Prediction of the Epidemic Peak of Coronavirus Disease in Japan, 2020. J Clin Med 2020; 9(3):789.
11. Chen, Z., Yang, J., and Dai, B. Forecast Possible Risk for COVID-19 Epidemic Dissemination Under Current Control Strategies in Japan. Int J Environ Res Public Health 2020; 17(11):3872.
12. Wang, X., Tang, T., Cao, L., Aihara, K., and Guo, Q. Inferring Key Epidemiological Parameters and Transmission Dynamics of COVID-19 Based on a Modified SEIR Model, Math Model Nat Phenom 2020; 15:74.
13. Kermack, W.O., McKendrick, A.G. A Contribution to the Mathematical Theory of Epidemics. Proc Roy Soc of London. 1927; Series A 115 (772):700−721.
14. Linton, N.M., Kobayashi, T., Yang, Y., Hayashi, K., Akhmetzhanov, A.R., Jung, S.M., et al. Incubation Period and Other Epidemiological Characteristics of 2019 Novel Coronavirus Serial Interval of Novel Coronavirus (COVID-19) Infections with Right Truncation: A Statistical Analysis of Publicly Available Case Data. J Clin Med 2020; 9(2):538.
15. Nishiura, H., Linton, N.M., Akhmetzhanov, A.R. Serial Interval of Novel Coronavirus (COVID-19) Infections. Int J Infect Dis 2020; 93:284-286.

16. Galmiche, S., Cortier, T., Charmet, T., Schaeffer, L., Cheny, O., von Platen, C., et al., SARS-CoV-2 incubation period across variants of concern, individual factors, and circumstances of infection in France: a case series analysis from the ComCor study. Lancet Microbe 2023;4(6):409-417.

17. Results of COVID-19 Vaccine Effectiveness Studies: An Ongoing Systematic Review, Forest Plots: Vaccine Effectiveness against Omicron Variant of Concern, Updated October 23, 2023. Available from:https://view-hub.org/sites/default/files/2023-10/COVID19%20VE%20Studies_Forest%20Plots_Omicron.pdf.

18. Feikin, D.R., Higdon, M.M., Andrews, N., Collie, S., Knoll, M.D., Kwong, J.C., et al. Assessing COVID-19 vaccine effectiveness against Omicron subvariants: Report from a meeting of the World Health Organization. Vaccine 2023;41(14):2329–2338.

19. [Tokyo Metropolitan Government Inspection System Improvement Plan for New Coronavirus Infection (Revised April 28, 2022)] (In Japanese). Available from: https://www.hokeniryo.metro.tokyo.lg.jp/kansen/kensa/kensakeikaku_kaitei_202204.files/keisataiseibikeikaku220428.pdf.

20. [Ministry of Health, Labor and Welfare. Reports on New Coronavirus Infections. OTC Availability of Medical Antigen Qualitative Test Kits, Devices and In Vitro Diagnostic Medical Devised Council 4th Meeting Reports 1-3, 17, Aug. 2022] (in Japanese). Available from: https://www.mhlw.go.jp/stf/newpage_27434.html.